Crack nucleation at the surface of stressed fibers

Document status and date:
Published: 01/01/1988

Document Version:
Publisher's PDF, also known as Version of Record (includes final page, issue and volume numbers)

Please check the document version of this publication:

• A submitted manuscript is the version of the article upon submission and before peer-review. There can be important differences between the submitted version and the official published version of record. People interested in the research are advised to contact the author for the final version of the publication, or visit the DOI to the publisher's website.
• The final author version and the galley proof are versions of the publication after peer review.
• The final published version features the final layout of the paper including the volume, issue and page numbers.

[Link to publication](#)

Download date: 04. Oct. 2023

Crack nucleation at the surface of stressed fibers

P. C. P. Bouten[a] and G. de With[b]

Philips Research Laboratories, P. O. Box 80.000, 5600 JA Eindhoven, The Netherlands

A model is proposed for crack initiation on a pristine surface. In this model failure starts from a flat surface and the crack develops during the strength or lifetime experiment. Both energy and kinetic arguments are used. The model is applied to lifetime calculations of pristine optical fibers. Surface energy and bulk elastic energy are calculated for a fiber with a flat and a slightly distorted surface. When a small amount of elastic energy is removed locally from the fiber, e.g., by dissolution, the distorted state is more stable. Like cracks in brittle materials, the stable distortions for pristine optical fibers have local radii of curvature at atomic dimensions. In this model the lifetime of a pristine fiber is mainly determined by the time needed to pass from a flat surface to a relatively small surface distortion. From the derived expression for the lifetime, the exponent n in the empirical power law expression for subcritical crack growth can be interpreted. It is shown that n is stress dependent. The discrepancy in n value observed for silica glass fibers ($n \simeq 20$) and bulk fused silica ($n \simeq 40$) is removed.

I. INTRODUCTION

In fracture mechanics it is an accepted view that existing flaws or cracks are responsible for failure of brittle materials.[1,2] Given a crack of length c and an applied stress σ_a, the stress intensity factor K_I is defined as

$$K_I = Y\sigma_a \sqrt{c}. \tag{1}$$

The geometrical constant Y is determined by the shape of the crack. With the applied stress normal to the crack plane, failure occurs at $K_I = K_{Ic}$, the fracture toughness. At stress intensities $K_I < K_{Ic}$, stress corrosion produces slow crack growth.[1] Given slow crack growth, the crack length at failure c_f is longer than the initial length c_i. The initial crack length is estimated from experiments where the slow crack growth is minimized, for instance, in liquid nitrogen,[3] in a vacuum,[4] in a dry atmosphere, or at high stress rate.

Preventing mechanical damage is important in the production of optical fibers. Many experimental results on strength and lifetime of undamaged optical fibers are reported. The tensile strength of these pristine fused silica fibers in ambient environment is about 5 GPa.[5] This corresponds to a strain at failure of 6%. Using the fracture toughness for fused silica, $K_{Ic} = 0.75$ MPa m$^{1/2}$, a final crack length at failure $c_f = 13$ nm ($Y = 1.26$; see Ref. 2) is obtained for the pristine fibers.

In vacuum or liquid nitrogen, larger fracture strains (14%–21%) are determined.[3,4] The corresponding initial crack length c_i is about 3 nm.

Under constant experimental conditions, the variation in fracture load of pristine optical fibers is only a few percent. Kurkjian and Peak related this to fiber diameter fluctuations.[6] Due to the small variations in strength, the fiber must have initial cracks of well-defined length (c_i) and shape (Y). In practice this means that initial cracks on the

pristine fiber have a length equal to about 10 atomic distances. The variation in length is less than 0.2 atomic distance. All initial cracks are thus very similar in shape and depth. This seems to be a nonrealistic model.

In the present paper a new model is presented for the description of the strength of fibers. This model contains both a stability criterion, comparable to the Griffith criterion, and a kinetic description, comparable to conventional stress-assisted corrosion behavior. As far as stability is concerned, suppose that no initial crack at all is present on the pristine fiber. The initial state, a flat surface, is well defined. Is it possible to develop a crack starting from this surface? This question is treated in Secs. II–IV of this paper. The (in)stability of a surface distortion at high stress levels is studied. The total energy of the distorted state is compared with that of the initial state. In the total energy, the elastic energy, the surface energy, the work, and possible heat of dissolution are taken into account. Two types of distorted state will be treated. In Sec. II, a surface distortion is made by moving material within the distorted section. The total volume is kept constant. The mechanism of material transport is irrelevant in this discussion. In Sec. III a surface distortion is described where some material is removed locally, e.g., by dissolution. The application of the stability criterion to the strength of optical fibers is discussed in Sec. IV.

Now consider the kinetic aspects. How fast will a distortion, stable with respect to the initial state, grow? This aspect is treated in Sec. V for a stress-assisted dissolution reaction. For the case of SiO_2, an often-used overall dissolution/corrosion reaction is given by

$$\equiv Si - O - Si \equiv + H_2O \rightarrow 2 \equiv Si - OH.$$
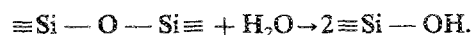
The rate v of the reaction is described with the expression for a stress-assisted reaction rate[7,8]:

$$v = v_0 \exp[(-E_a + V\sigma_l)/RT], \tag{2}$$

where E_a is the activation energy at zero stress, V the activation volume, σ_l the local stress, R the gas constant, and T the

---

[a] Present address: Philips Centre for Manufacturing Technology, P. O. Box 218, 5600 MD Eindhoven, The Netherlands.
[b] Also affiliated with Eindhoven University of Technology.

temperature. The effective activation energy $E_{\mathrm{act}} = E_a - V\sigma_l$ is lowered by the stress. For fracture the chemical bond has to be greatly elongated. Under external stress, a part of the elongation is already made. Therefore, the activation energy to be surmounted is lower.[7,8] High reaction velocities are obtained at high local tensile stresses.

Due to this stress-activated reaction, a distortion becomes larger. It can grow to a crack, with a length c that is large compared with the radius ρ of the tip. When a reaction path is known, the failure time can be calculated. As a consequence of these kinetic aspects it is shown in Sec. VI that the fatigue parameter n, often used to describe slow crack growth, is an improper parameter. Finally, in Sec. VII, a comparison with conventional theories and some limitations of the present model are discussed.

II. STABILITY WITH MATERIAL DISPLACEMENT

A. Surface distortion

A perfect fiber of radius r_0 has a smooth surface. A force F_a is applied along the axis. Due to an unspecified process, some material is displaced within a certain part of the fiber. The diameter of the fiber thus varies slightly with the position on the fiber axis. The total energy of this distorted system, consisting of elastic energy and surface energy, is now calculated. From the total energy it can be seen when a distorted state is stable with respect to the initial state.

Within a distorted region of length Λ (Fig. 1), a sinusoidal distortion is assumed. The fluctuation of local radius r along the fiber axis z is given as

$$r = r_0 [1 + x \cos(\omega z) - (x^2/4)], \tag{3}$$

where $x = a/r_0$ is the normalized depth of the fluctuation and $\omega = 2\pi/\Lambda$. The term in x^2 is necessary to keep the total volume constant.

B. Surface energy

The area A_Λ of the curved surface segment is
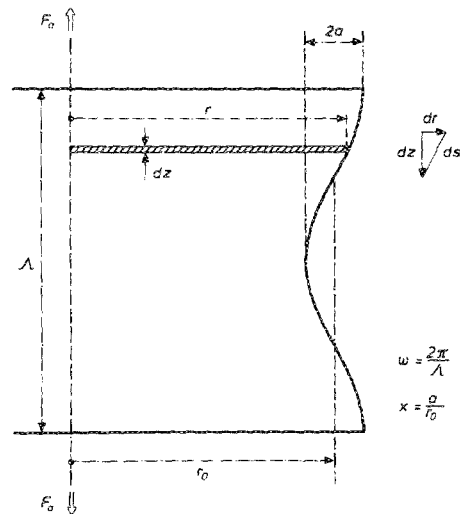

FIG. 1. Geometry of the fiber section with a sinusoidal surface distortion. The volume of the distorted section remains constant. F_a is the applied force, Λ the deformation length, $2a$ the depth, and r_0 the initial fiber radius. The normalized depth x and reciprocal length ω are used in the calculations.

$$A_\Lambda = \int_0^\Lambda 2\pi r\, ds = \int_0^\Lambda 2\pi r \sqrt{1 + \left(\frac{dr}{dz}\right)^2}\, dz$$

$$= 2\pi r_0 \int_0^\Lambda \left(1 + x \cos(\omega z) - \frac{x^2}{4} \right)$$

$$\times \sqrt{1 + [x r_0 \omega \sin(\omega z)]^2}\, dz. \tag{4}$$

The second term in this integral expression, containing the cosine term, gives zero. An analytical solution for the remaining integral is, to our knowledge, not possible. For small values of $x r_0 \omega (= 2\pi a/\Lambda)$, the square root can be approximated. Then Eq. (4) leads to

$$A_\Lambda \simeq 2\pi r_0 \Lambda [1 + (k - \tfrac{1}{4}) x^2], \tag{5}$$

with

$$k = (\pi r_0 / \Lambda)^2. \tag{6}$$

For $2\pi a/\Lambda < 0.75$, the difference between the numerically calculated exact solution of Eq. (4) and approximation (5) is less than 1%. For $2\pi a/\Lambda = 2$, the surface area is overestimated by 19%.

The surface energy of the system becomes

$$U_{\mathrm{surf}} \simeq \gamma A_\Lambda = 2\pi r_0 \Lambda \gamma [1 + (k - \tfrac{1}{4}) x^2], \tag{7}$$

where γ is the specific surface energy of the fiber material.

C. Elastic energy

For a fiber of radius r, the stress σ is calculated from the applied force F_a:

$$\sigma = F_a / \pi r^2. \tag{8}$$

This relation is used for the stress in the fiber segment with a small surface distortion ($2\pi a < \Lambda$). Stress concentration is not taken into account. The material follows Hooke's law,[9] $\sigma = \epsilon E$ (ϵ is the strain and E is Young's modulus).

In a fiber segment of length dz and radius r (Fig. 1) the elastic energy is

$$dU_{\mathrm{el}} = (\sigma^2/2E)\pi r^2\, dz. \tag{9}$$

The elastic energy in the described fiber segment of length Λ is then

$$U_{\mathrm{el}} = \int_0^\Lambda \frac{\pi r^2 F_a^2}{2E(\pi r^2)^2}\, dz$$

$$= \frac{F_a^2}{2\pi r_0^2 E} \Lambda \frac{1 - (x^2/4)}{\{[1 - (x^2/4)]^2 - x^2\}^{3/2}}. \tag{10}$$

Equations (3) and (8) were used in the derivation.

The strain ϵ of the distorted fiber section Λ is

$$\epsilon = \frac{1}{\Lambda} \int_0^\Lambda \epsilon_z\, dz = \frac{1}{\Lambda} \int_0^\Lambda \frac{F_a}{\pi r^2 E}\, dz$$

$$= \frac{F_a}{\pi r_0^2 E} \frac{1 - (x^2/4)}{\{[1 - (x^2/4)]^2 - x^2\}^{3/2}}. \tag{11}$$

At constant strain ($d\epsilon/dt = 0$), the force F_a to be applied depends on the relative depth x of the fluctuation:

$$F_a = F_0 \frac{\{[1 - (x^2/4)]^2 - x^2\}^{3/2}}{[1 - (x^2/4)]}, \tag{12}$$

where F_0 is the force applied to an undistorted fiber.

The elastic energy of the fiber at constant strain then becomes

$$U_{el} = \frac{\sigma_{a,0}^2}{2E} V_0 \frac{\{[1 - (x^2/4)]^2 - x^2\}^{3/2}}{[1 - (x^2/4)]} \qquad (13)$$

$$(\sigma_{a,0} = F_0/\pi r_0^2; \quad V_0 = \pi r_0^2 \Lambda).$$

D. Total energy

For the total energy of the system, two cases must be distinguished: constant force and constant strain. For constant force, the strain (11), and therefore the displacement, changes with increasing deformation depth. Besides the elastic energy and the surface energy, a work term is required. At constant strain, no work term appears in the total energy because there is no overall displacement. In that case the total energy is

$$U_{tot} = U_{surf} + U_{el}. \qquad (14)$$

The reduced energy U_r is defined as

$$U_r = (2E/\sigma_{a,0}^2 V_0) U_{tot}. \qquad (15)$$

Then

$$U_r = \frac{\{[1 - (x^2/4)]^2 - x^2\}^{3/2}}{[1 - (x^2/4)]} + Q[1 + (k - \tfrac{1}{4})x^2], \qquad (16)$$

with

$$Q = 4\gamma E/r_0 \sigma_{a,0}^2. \qquad (17)$$

For small x the reduced energy is a continuously increasing function in x when $Q(k - 1/4) > 2$. With reasonable estimates for γ, E, $\sigma_{a,0}$, and r_0 (see Sec. IV), the presented model has no minimum when distortion length $\Lambda < 1$ μm. This means that a small surface distortion due to material displacement is not stable.

III. STABILITY WITH MATERIAL REMOVAL

A. Surface geometry

In the previous section the amount of material within the distorted part of the fiber remained constant. We now study the case where some material is removed at the distortion, leading to a local decrease of the radius (Fig. 2):

$$r = r_0[(1 - x) + x \cos(\omega z)]. \qquad (18)$$

Note that this expression differs slightly from Eq. (3).

The total energy expression has to be taken into account, not only the elastic energy and the surface energy, but also the energy used to remove the material. In the case of dissolution, this is heat of dissolution.

B. Heat of dissolution

The heat of dissolution is proportional to the dissolved volume V_d. The volume of the removed cylindrical section (Fig. 2) is

$$V_d = \int_0^\Lambda \pi(r_0^2 - r^2) dz = V_0(2x - 1.5x^2), \qquad (19)$$

where $V_0 = \pi r_0^2 \Lambda$ is the total volume of the cylindrical section. The total energy contribution due to this heat of dissolution is then
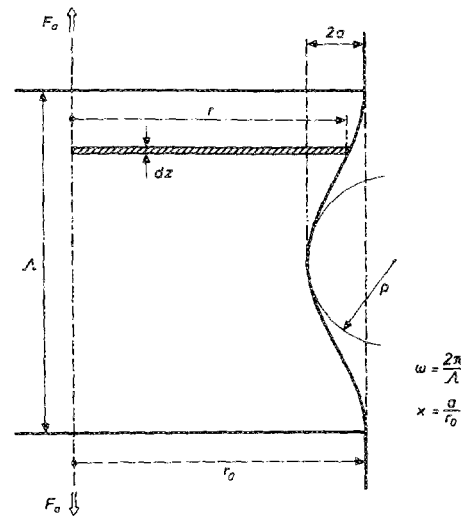

FIG. 2. Geometry of the fiber section with a sinusoidal surface distortion. At the distortion material is removed. The fiber initial radius is r_0. Tip radius ρ is defined at the middle of the distortion.

$$U_{diss} = (V_d/V_m)H = (V_0/V_m)(2x - 1.5x^2)H, \qquad (20)$$

where H is the molar heat of dissolution and V_m the molar volume of the fiber material.

C. Surface energy and elastic energy

In the same way as in Sec. II B, but starting from expression (18) instead of (3) for the description of the distortion, the surface energy U_{surf} of the fiber segment is

$$U_{surf} = \gamma A_\Lambda = 2\pi r_0 \Lambda \gamma[(1 - x)(1 + kx^2)]. \qquad (21)$$

Using expressions (9) and (18), the elastic energy of the section Λ of the fiber (Fig. 2) is

$$U_{el} = \frac{F_a^2}{2\pi r_0^2 E} \int_0^\Lambda \frac{dz}{[(1 - x) + x \cos(\omega z)]^2}$$

$$= \frac{F_a^2}{2\pi r_0^2 E} \Lambda \frac{1 - x}{(1 - 2x)^{3/2}}. \qquad (22)$$

In analogy with Eq. (11), the overall strain becomes in this case

$$\epsilon = \frac{F_a}{\pi r_0^2 E} \frac{1 - x}{(1 - 2x)^{3/2}}. \qquad (23)$$

At constant strain, the force decreases with increasing depth x. Starting with force F_0 at zero depth,

$$F_a = F_0[(1 - 2x)^{3/2}/(1 - x)]. \qquad (24)$$

The elastic energy in the segment with length Λ and relative distortion depth x is thus for the present case, at constant strain,

$$U_{el} = \frac{F_0^2}{2\pi r_0^2 E} \Lambda \frac{(1 - 2x)^{3/2}}{(1 - x)} = \frac{\sigma_{a,0}^2}{2E} V_0 \frac{(1 - 2x)^{3/2}}{(1 - x)}. \qquad (25)$$

For $x \ll 1$, a combination of (19) and (25) gives

$$U_{el} = (\sigma_{a,0}^2/2E)(V_0 - V_d). \qquad (26)$$

The change in elastic energy is in that case equal to the elastic

energy that was present in the removed volume before the surface was distorted.

D. Total energy

As in Sec. II D, only the case for constant strain is treated. The total energy is then

$$U_{tot} = U_{el} + U_{surf} + U_{diss}. \tag{27}$$

Using (15), (17), (20), (21), and (25) and K for the ratio of the heat of dissolution and the elastic energy per unit volume,

$$K = 2EH/V_m \sigma_{a,0}^2, \tag{28}$$

the reduced total energy is

$$U_r(x) = [(1-2x)^{3/2}/(1-x)] + Q(1-x)(1+kx^2)$$
$$+ K(2x - 1.5x^2). \tag{29}$$

In Sec. IV (Table I), typical values for Q and k will be given: $Q \ll 1$, $k \gg 1$, and $x \ll 1$. The magnitude of the product Qkx is about 1.0. Figure 3 shows this total (reduced) energy U_r for $x \ll 1$ and $K = 0$. The elastic energy decreases, and the surface energy increases with depth x. The total energy has a minimum.

At $K = 1$ and $x \ll 1$, $U_{el} + U_{diss} = 0$. It is easy to show that for $K > 1$ no minimum exists.

The position of the minimum is obtained from $dU_r/dx = 0$. For the noted conditions ($x \ll 1$, $Q \ll 1$, $Qk \gg 1$, $K < 1$),

$$x_{min} = (1-K)/Qk \tag{30}$$

is obtained.

A limiting case for the reaction is the situation in which the total energy remains constant. $\Delta U_r = U_r(0) - U_r(x) = 0$ [Eq. (29)] has, under the same conditions, a solution at

$$x_0 = 2(1-K)/Qk. \tag{31}$$

TABLE I. Some values used in the models presented in Secs. II and III. A tensile loaded fused silica optical fiber serves as model system.

| Values used in the calculation			
Fiber:	radius		$r_0 = 62.5 \mu m$
	applied stress		$\sigma_a = 4.0$ GPa
Fused silica:	molar volume		$V_m = 27.3$ cm^3
	Young's modulus		$E = 72$ GPa
	surface energy		$\gamma = 0.2$ J/m^2
Heat of solution			$H = 0.0$ kJ/mol
Typical deformation depth			$a = 0.5$ nm
Calculated:			
	constants		$Q = 5.76 \times 10^{-5}$
			$K = 0$
	relative depth		$x = 8.0 \times 10^{-6}$
With material removed (Sec. III):			
at minimum energy:			
	deformation length		$\Lambda = 4.2$ nm
	tip radius		$\rho_{min} = 0.90$ nm
			$k = 2.17 \times 10^9$
at zero energy change:			$\Lambda = 3.0$ nm
			$\rho_0 = 0.45$ nm
			$k = 4.34 \times 10^9$
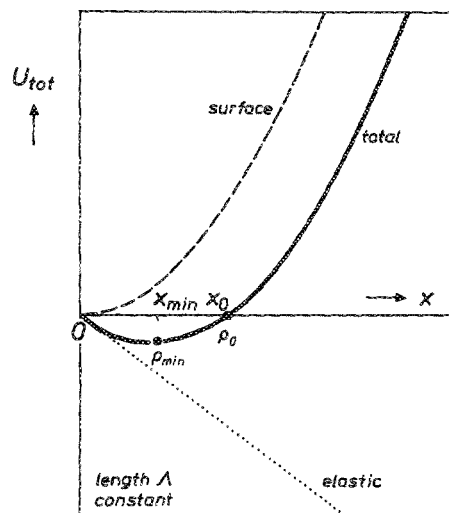
FIG. 3. Energy as a function of the deformation depth x, when material is removed. The length Λ is constant. The elastic energy (dotted curve) and the surface energy (dashed curve) give the total energy (solid curve). The minimum in total energy corresponds with deformation depth x_{min} and tip radius ρ_{min}. At zero energy the depth x_0 corresponds with radius ρ_0.

Figure 3 shows clearly that for a given length Λ the total energy increases for $x > x_0$.

E. Radius of curvature

The local radius of curvature ρ on a curve $y(x)$ is defined as[10]

$$\rho = \left[1 + \left(\frac{dy}{dx}\right)^2\right]^{3/2} \Big/ \left(\frac{d^2y}{dx^2}\right). \tag{32}$$

In the middle of the distortion, at $z = \Lambda/2$ [Eqs. (3) and (18), Figs. 1 and 2],

$$\rho = \Lambda^2/4\pi^2 a. \tag{33}$$

At $x = x_{min}$ (Fig. 3), the total energy has a minimum. The local radius of curvature in the middle of the distortion is

$$\rho_{min} = \gamma E/\sigma_{a,0}^2(1-K). \tag{34}$$

At $x = x_0$ there is no energy change with respect to the initial state. The local radius of curvature is

$$\rho_0 = \gamma E/2\sigma_{a,0}^2(1-K) = \rho_{min}/2. \tag{35}$$

At minimum total energy and at zero energy change, the local radii of curvature at the tip [Eqs. (34) and (35)] are independent of the depth and the length of the distortion. This is true as long as the approximations for elastic energy and surface energy are valid, thus when $2\pi a \ll \Lambda$.

At $K = 1$, the decrease of the elastic energy of the fiber segment is equal to the (endothermic) heat of solution of the removed material. Then $\rho \to \infty$. The surface distortion is no longer stable; a fatigue limit is reached. From Eq. (28) this limit is

$$\sigma_{limit} = \sqrt{2EH/V_m} \quad (H > 0). \tag{36}$$

From Eqs. (34) and (35) it is clear that, for $K < 0$, distortions with still smaller local radii can be stable.

IV. DISCUSSION ON THE STABILITY

A. Type of distortion

In Secs. II and III, expressions for the total energy of a system with a surface distortion were derived. From these expressions, stability criteria are obtained. In this section, they are used for an optical fiber with radius $r_0 = 62.5$ μm (Table I). Fused silica has a Young's modulus $E = 72$ GPa and a molar volume $V_m = 27.3$ cm^3. In strength and lifetime experiments, the stress at fracture for a "perfect" optical fiber is between 2 and 6 GPa.[5,11] In this section, 4 GPa is taken as a typical value.

For SiO$_2$ glass, several values are reported for the surface energy γ. A siloxane surface (only Si-O-Si bridges) has a surface energy of about 0.26 J/m^2.[12] For the silanol surface it is about 0.13 J/m^2. The outer fiber surface may be a siloxane or silanol surface. As a typical value, $\gamma = 0.2$ J/m^2 is taken. In a fast fracture process, where dangling bonds are produced as an intermediate product, $\gamma = 4$ J/m^2 is used.[1] This estimate is inappropriate here.

From Sec. II it was concluded that no stable fluctuation was obtained for $Q(k - 1/4) > 2$. In Table I, $Q = 5.8 \times 10^{-5}$ is calculated. This implies that stable fluctuations are only possible for $\Lambda > 1.1$ μm. For a small distortion ($a = 0.5$ nm), the local tip radius is very large ($\rho > 56\mu$m).

For the stability with material removal (Sec. III), an estimate for H, e.g., the heat of solution, is needed. With $H = 0$ kJ/mol ($K = 0$), stable fluctuations with respect to the initial state are obtained for $\rho > \rho_0$ [Eq. (35)]. At $\sigma_{a,0} = 4$ GPa, $\rho_{min} = 0.9$ nm and $\rho_0 = 0.45$ nm (Table I). Having a distortion of small depth, e.g., $a = 0.5$ nm, lengths of $\Lambda = 4.2$ and 3.0 nm are derived for ρ_{min} and ρ_0, respectively [Eq. (33)].

The allowance of material removal stabilizes much shorter surface distortions. At comparable deformation depths they have much smaller radii of curvature at the tip. These surface distortions have local radii of curvature comparable to those of cracks in brittle solids.[13] The magnitude of the tip radius determines the local stress [Eq. (1)] and therefore the stress-corrosion rate [Eq. (2)]. In the following sections, only the case with material removal (Sec. III) is further treated. Within this formalism, stable fluctuations are obtained much easier than within the one with material displacement.

B. Comparison with the Griffith concept

In the calculation of the elastic energy (Secs. II C and III C), a constant stress over the cross section is assumed. This will be true for small distortions, thus $2\pi a/\Lambda < 1$. In the case presented this ratio is about 1 ($a = 0.5$ nm). Better solutions of the elastic problem are obtained when the changed stress situation around the crack is taken into account.

For the case of a sharp crack, this has been done by Griffith (see, e.g., Ref. 2). The total energy for a sharp internal crack of unit width and length $2c$ is

$$U_{tot} = -2\pi c^2(\sigma^2/2E) + 4\gamma c. \qquad (37)$$

This total energy has a maximum at $\sigma = \sqrt{2\gamma E/\pi c}$ (Fig. 4), the Griffith fracture condition. For $K_{Ic} = \sqrt{2\gamma E}$, it is identi-
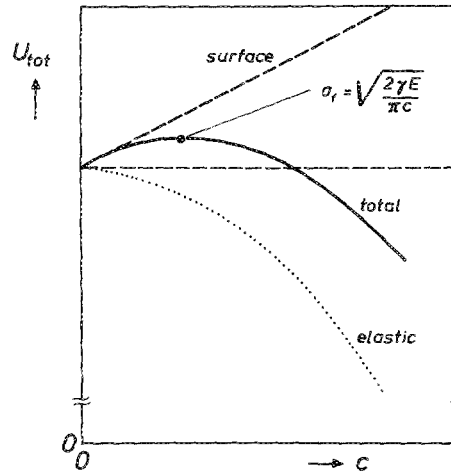

FIG. 4. Energy U_{tot} as a function of crack length c for a Griffith crack. The total energy has a maximum at the Griffith fracture condition. Starting at $c = 0$, the total energy has to increase before failure can occur.

cal to Eq. (1). For a surface crack of length c the geometrical factor Y differs slightly. With this sharp crack, the change in elastic energy is proportional to c^2. For large distortions ($2\pi a/\Lambda \gg 1$) this is much more than calculated in Eq. (26). In the total energy expression, the surface energy was overestimated for $2\pi a/\Lambda > 1$. From these arguments it is concluded that for $2\pi a/\Lambda > 1$ the calculated tip radii [Eqs. (34) and (35)] are too large and no longer constant.

C. Reaction velocity and energy decrease

A sinusoidal surface distortion of length Λ is energetically favorable with respect to a flat surface when $0 < x < x_0$ (Fig. 3). This means that the tip radius ρ has a lower limit: $\rho > \rho_0$. For increasing Λ the total energy curves are drawn in Fig. 5. For larger Λ, larger x_0 and x_{min} are obtained. The minima of these curves (constant tip radius ρ_{min}) are on a straight line ($x \ll 1$). The total energy of a deformation with
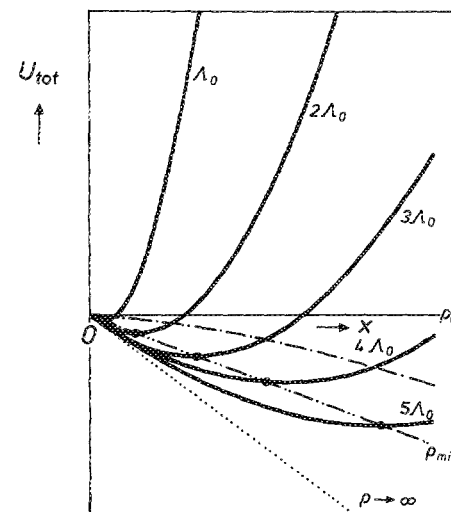

FIG. 5. Total energy curves of Fig. 3 for various deformation lengths (Λ_0–$5\Lambda_0$). For tip radii $\rho > \rho_0$, there is energy production when the distortion size increases. Starting at $x = 0$, a reaction path with continuously decreasing total energy is possible, e.g., the dot-dashed curve.

constant tip radius $\rho_{\min}$ decreases with increasing deformation depth. Size increase is energetically favorable. For a tip radius ρ_0 the total energy remains constant.

The reaction velocity [Eq. (2)] is larger for higher (local) stress. At constant applied stress, a smaller tip radius (at identical deformation depth) gives rise to a larger local stress. From the reaction velocity, the largest crack velocity is expected at the smallest tip radius. However, with too small tip radii ($\rho < \rho_0$) the increase in deformation size is energetically unfavorable: the total energy increases.

Working with total energy decrease and reaction velocity leads to a conflicting situation. In the first case the radius has a minimum, in the second case it does not. Neither the total energy decrease nor the reaction velocity alone can solve the problem. They have to be combined. The actual reaction path is determined by the entropy production rate.[14] While the process of material removal is not fully specified, the contribution of the entropy to the calculation of the reaction path is not incorporated. The calculation of the actual reaction path is outside the scope of this paper. In forthcoming calculations (Sec. V) of the lifetime it is assumed that a maximum energy release rate determines the reaction path. Energy is only produced for $\rho > \rho_0$. For small ρ, the amount of energy produced with an increase of the deformation depth is smaller than at larger ρ. For larger ρ, the reaction rate is slower. The actual reaction path can be drawn in Fig. 5 as a line of continuously decreasing total energy with increasing depth x. Comparing this with Fig. 4, the Griffith concept, leads to a clear conclusion:

In Griffith's model, a flat surface of a stressed sample is stable with respect to a short crack. For failure, a crack nucleation step with higher total energy is needed. The model presented in this chapter does not need such a nucleation step. This is illustrated in Fig. 6. Under tensile stress, the flat surface is an unstable state if a mechanism is present to remove locally some material, and thereby some elastic energy from the matrix. The essential difference between the two models is the allowance of material removal.

V. KINETIC ASPECTS

A. Local stress and reaction velocity

The sinusoidal surface distortion (Fig. 2) can be described with depth $2a$ and tip radius ρ. The local stress at the tip of this distortion is approximated by Inglis' relation

$$\sigma_l = \sigma_a \left[1 + 2\sqrt{(c/\rho)} \right], \qquad (38)$$

where $c = 2a$, σ_a is the applied stress, and σ_l is the local stress. The velocity of a stress-assisted reaction is described with Eq. (2). Due to stress concentration, the local stress at the tip of a distortion is larger than on a flat surface. At this tip the reaction is faster; the size of the distortion increases.

The failure time is the time needed for the formation of a critical crack. A critical crack is reached when $K_I = Y\sigma_a \sqrt{c}$ equals K_{Ic}. In the calculation of the failure time we start from a flat surface. Most of the time is spent at low reaction velocities, when the stress concentration at the crack tip is small ($2\pi a/\Lambda < 1$). For the calculation of the failure time in this case, the behavior of ρ for large distortions ($2\pi a/\Lambda > 1$) is not important.
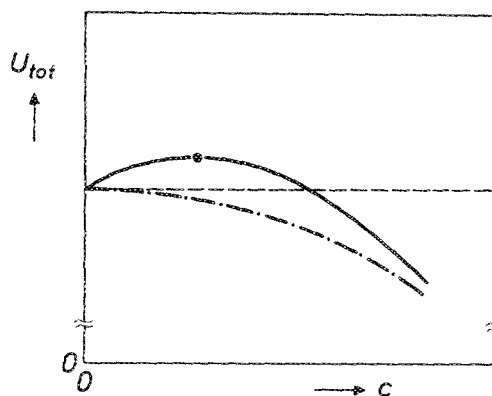

FIG. 6. Total energy of Griffith's model (Fig. 4), compared with an estimated reaction path at continuously decreasing energy. This is a path between the zero total energy change at ρ_0 and maximum total energy decrease, indicated in Fig. 5 (dot-dashed curve).

Combining the reaction velocity v [Eq. (2)] and stress concentration [Eq. (38)] gives

$$v = \frac{dc}{dt} = v_1 \exp(D_v \sqrt{c}), \qquad (39)$$

where

$$v_1 = v_0 \exp\left[(-E_a + V\sigma_a)/RT \right] \qquad (40)$$

and

$$D_v = 2V\sigma_a/RT\sqrt{\rho}. \qquad (41)$$

σ_a is the applied stress, E_a the zero stress activation energy of the stress corrosion reaction, V the activation volume, and R the gas constant. Note that D_v is not necessarily constant during the reaction; it depends on ρ.

For cracks in brittle materials, $c \gg \rho$. The first term in Inglis' relation [Eq. (38)] is then neglected. In that case, using $K_I = Y\sigma_a \sqrt{c}$ (1), Eq. (39) can be written as

$$v = v_0 \exp\left[(-E_a + bK_I)/RT \right], \qquad (42)$$

where

$$b = 2V/Y\sqrt{\rho}. \qquad (43)$$

Expression (42) is often used to describe slow crack growth in brittle materials like glass.[15,16] Usually b is assumed to be a constant. In the Inglis formalism [Eq. (38)] failure occurs if the crack tip stress exceeds the theoretical strength σ_{th}. For fused silica, $\sigma_{th} \simeq 20$ GPa.[17] Using the stress intensity factor [Eq. (1)], spontaneous failure occurs when $K_I > K_{Ic}$. A combination of these formalisms gives for large cracks ($c \gg \rho$)

$$b = V\sigma_{th}/K_{Ic}. \qquad (44)$$

For slow crack growth experiments on fused silica in water of various temperatures Wiederhorn and co-workers[15,16] report $b = 0.216$ mol m$^{5/2}$. Using Eq. (44) and $K_{Ic} = 0.75$ MPa m$^{1/2}$, an activation volume $V = 8.1$ cm^3/mol is obtained.

In the present study it is assumed that no initial cracks are present; Eq. (39) is used. The reaction rate is fast for small ρ. For too small ρ, the total energy of the system increases. This is unfavorable. Therefore, two cases can be distinguished.

(1) The (initial) dissolution rate at the tip of the distortion is so fast that the tip radius will become very small. This is energetically forbidden; $\rho > \rho_0$. Then the necessary total energy decrease limits the reaction velocity at the tip. To hold the tip radius above ρ_0, the dissolution rate beside the actual tip is important. This (lower) velocity determines the rate at which the depth a of the distortion increases.

(2) In the opposite case, the local radius is larger than ρ_0. The dissolution at the tip is the rate-determining step. The reaction rate at the tip is kinetically determined.

Intermediate between cases (1) and (2) is when the dissolution rate at the tip determines the crack growth, but the tip radius ρ remains constant. For this case expressions for the failure time are derived in the next sections.

B. Lifetime for constant tip radius and zero initial depth

Assume that the tip radius is constant at $\rho = \rho_0$ and the lifetime is only determined by the reaction velocity at the crack tip. The total energy of the system then does not change. Using Eq. (39), the time to failure is given by

$$t_f = \int_{c_i}^{c_f} \frac{1}{dc/dt} \, dc = \frac{1}{v_1} \int_{c_i}^{c_f} \exp(-D_v \sqrt{c}) dc. \quad (45)$$

Taking $u = D_v \sqrt{c}$,

$$t_f = \frac{2}{v_1 D_v^2} \int_{u_i}^{u_f} u \exp(-u) du$$

$$= \frac{2}{v_1 D_v^2} \left[-(1+u)\exp(-u)|_{u_i}^{u_f} \right]. \quad (46)$$

Spontaneous failure occurs when the local stress is equal to a critical stress σ_{crit}, for instance, the theoretical strength σ_{th}. This is the case when

$$u_f = D_v \sqrt{c_f} = (V/RT)(\sigma_{\text{crit}} - \sigma_a). \quad (47)$$

For the special case that the initial state is a flat surface ($u_i = 0$), Eq. (46) gives

$$t_f = \frac{2}{v_1 D_v^2} \left[1 - \left(1 + \frac{V}{RT}(\sigma_{\text{crit}} - \sigma_a) \right) \right.$$

$$\left. \times \exp\left(-\frac{V}{RT}(\sigma_{\text{crit}} - \sigma_a) \right) \right]. \quad (48)$$

The term in square brackets deviates less than 1% from 1.0 when $[V(\sigma_{\text{crit}} - \sigma_a)/RT] > 6.6$. For an activation volume V of 8 cm^3/mol this agrees with $(\sigma_{\text{crit}} - \sigma_a) > 2.0$ GPa. When $\sigma_{\text{crit}} = \sigma_{\text{th}}$, this is easily achieved in practical situations. For the theoretical strength, a value of about 20 GPa is reported. In ambient environment, failure stresses up to 6 or 7 GPa are reported on fibers. Only in vacuum or liquid-nitrogen higher fracture stresses (or strains) are reported.[3,4] The term in square brackets is thus safely approximated with 1. Then

$$t_f = 2/v_1 D_v^2. \quad (49)$$

Using expression (35) for tip radius ρ_0 and σ_a for $\sigma_{a,0}$ this is rewritten as

$$\ln(t_f) = -\frac{V}{RT}\sigma_a - 2\ln\sigma_a - \ln\left(\sigma_a^2 - \frac{2EH}{V_m} \right)$$

$$+ \frac{E_a}{RT} + \ln\left[\left(\frac{RT}{V} \right)^2 \frac{\gamma E}{4v_0} \right]. \quad (50)$$

Defining the calculated activation volume V_{calc} as

$$V_{\text{calc}} = -RT \frac{d \ln t_f}{d\sigma_a}, \quad (51)$$

Eqs. (28) and (50) result in

$$V_{\text{calc}} = V + \frac{2RT}{\sigma_a}\left(\frac{2-K}{1-K} \right). \quad (52)$$

It is only defined for $K < 1$. The calculated activation volume is always larger than V for the chemical reaction. For $K = 1$, $V_{\text{calc}} \to \infty$; a fatigue limit exists. For $K = 0$ it gives

$$V_{\text{calc}} = V + (4RT/\sigma_a). \quad (53)$$

The stress dependence of V_{calc} is a consequence of the stress dependence of the (minimum) radius of curvature [Eqs. (34) and (35)] and the stress dependence of the critical crack length c_f.

Using $\rho_{\text{min}} = 2\rho_0$ instead of ρ_0 as a constant radius of curvature in the calculation of t_f, the lifetime is only twice that given in Eq. (48), since t_f is proportional to D_v^{-2}, thus linearly dependent on ρ. The expression for V_{calc} remains the same.

C. Lifetime at nonzero initial distortion depth

More in general, when a small surface distortion, defined by c_i and ρ_i, was previously present, and $\sqrt{c_i/\rho_i} \ll \sqrt{c_f/\rho_f}$, it follows from Eq. (45) (for $2\pi a/\Lambda < 1$, thus $c_i < \rho_i$) that

$$t_f = (2/v_1 D_v^2)\left[(1 + D_v \sqrt{c_i})\exp(-D_v \sqrt{c_i}) \right], \quad (54)$$

where $D_v = (2V\sigma_a)/(RT\sqrt{\rho_i})$. In this case the term in square brackets is stress dependent. For $K = 0$ this expression gives

$$t_f = \frac{2\rho_i}{4v_0}\left(\frac{RT}{V} \right)^2 \frac{1}{\sigma_a^2} \left[\left(1 + 2\frac{V\sigma_a}{RT}\sqrt{\frac{c_i}{\rho_i}} \right) \right.$$

$$\left. \times \exp\left(\frac{E_a - V\sigma_a(1 + 2\sqrt{c_i/\rho_i})}{RT} \right) \right]. \quad (55)$$

Two different cases are treated here. For case (1) the tip radius remains constant and equal to ρ_i. The term outside the square brackets is proportional to $1/\sigma_a^2$. For case (2) the initial tip radius depends on the stress as was used in previous sections [Eqs. (34) and (35)]. For this stress dependence of ρ the term outside the square brackets is proportional to $1/\sigma_a^4$. For both cases Eq. (55) may be rewritten as

$$\ln(t_f) = \frac{E_a}{RT} - \frac{V}{RT}\sigma_a\left(1 + 2\sqrt{\frac{c_i}{\rho_i}} \right) - q\ln\sigma_a + 2\ln T$$

$$- \ln v_0 + \ln\left(1 + 2\frac{V}{RT}\sigma_a\sqrt{\frac{c_i}{\rho_i}} \right) + P. \quad (56)$$

In this equation the constants P and q differ for the two cases. For case 1, $q = 2$ and $P = \rho_i R^2/2V^2$. For case 2 [and Eq. (35)], $P = \gamma E(R/2V)^2$ and $q = 4$.

When the ratio

$$X_i = \sqrt{c_i/\rho_i}, \qquad (57)$$

thus the initial crack geometry is known and the lifetime is determined. The calculated activation volume V_{calc} [Eq. (51)] is determined from the stress dependence of the lifetime [Eq. (56)] for a given depth X_i:

$$V_{\mathrm{calc}} = V(1 + 2X_i) + \frac{RT}{\sigma_a}\left(\frac{q + 2(q-1)(V\sigma_a/RT)X_i}{1 + 2(V\sigma_a/RT)X_i}\right). \qquad (58)$$

This expression shows clearly that the slope of the lifetime plot ($\sigma_a \leftrightarrow \ln t_f$), expected from the theory, is strongly dependent on the initial crack geometry. This dependence is mainly determined by the first term of Eq. (58). The magnitude of the term in large parentheses varies between q and $(q-1)$, dependent on the magnitude of $(V\sigma_a/RT)X_i$.

VI. FATIGUE CONSTANT n: THE WRONG PARAMETER

The fatigue parameter n, often used to describe slow crack growth phenomena and fatigue data, was introduced by Charles.[18] It is used in the power law $v = AK_I^n$, where v is the crack velocity, K_I the stress intensity [Eq. (1)], and A a constant.[1] From the power law it is easy to show that the lifetime $t_f \sim 1/\sigma_a^n$, where σ_a is the applied stress. Then n can be determined from a plot of $\ln t_f$ as a function of $\ln \sigma_a$:

$$n = -\frac{d \ln t_f}{d \ln \sigma_a}. \qquad (59)$$

A value of $n = 20$ is often obtained from strength and lifetime measurements on pristine silica fibers, and is treated as a typical value. From slow crack growth experiments on bulk fused silica, $n \simeq 40$ is obtained.[15,19] A discrepancy between the n values of optical fibers and cracks in fused silica is observed.

The use of Eq. (59) in combination with the lifetime equation (56) at a distortion of depth $X_i = (c_i/\rho_i)^{1/2}$ results in

$$n = \frac{V\sigma_a}{RT}(1 + 2X_i) + \left(\frac{q + 2(q-1)(V\sigma_a/RT)X_i}{1 + 2(V\sigma_a/RT)X_i}\right). \qquad (60)$$

The expression in large parentheses is the same as in Eq. (58). It is shown that the fatigue parameter n and the activation volume V are closely related. For this relation the magnitude of $\sigma_a(1 + 2X_i)$ has to be known. From Inglis' relation (38) it is seen that this is the local stress σ_l at the tip of the deformation. This means that the fatigue parameter n depends on the magnitude of σ_l. The first term of Eq. (60) becomes $V\sigma_l/RT$. The term in large parentheses can vary between 1 and 4.

In Fig. 7 values for n [Eq. (60)] are given for $V = 8.1$ cm^3/mol, $T = 293$ K, and various values of the local stress σ_l. The initial depth X_i is the variable. The failure stress of a pristine fiber is in the range of 2–6 GPa.[5,6,11] Using $V = 8.1$ cm^3/mol, obtained from slow crack growth data, V_{calc} describes well the experimental data on pristine fibers represented by $n = 20$. The value of $V = 8.1$ cm^3/mol, however, is obtained from slow crack growth data on longer cracks [Eq.
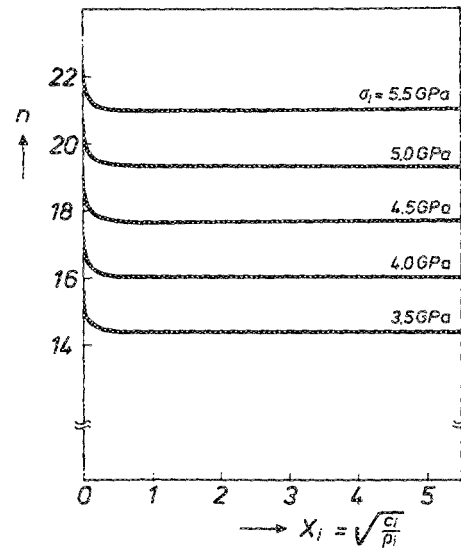

FIG. 7. Calculated values of fatigue constant n for several values of local stress σ_l and variable initial length X_i. This calculation is made for $V = 8.1$ cm^3/mol and $q = 4$ at $T = 293$ K.

(44)], giving in the power-law description a value of $n = 40$. Thus, the stress corrosion of pristine fused silica (optical) fibers at high stress and of cracks in bulk silica can be described with the same activation volume. In other words, $n = 20$ for pristine optical fibers and $n = 40$ for large cracks in fused silica agree with each other since n is not the proper parameter. Expression (60) resolves the discrepancy in n values as observed for bulk fused silica glass and their fibers.[20] The activation volume is defined as the difference in molar volume between the initial state and the state prior to fracture.[8] Since the strain at failure for the inert strength is about 0.2, a rough estimate of the activation volume is about $0.2 V_m \simeq 6$ cm^3/mol. This is consistent with the experimental value of 8.1 cm^3/mol.

VII. GENERAL DISCUSSION

A. On the reaction path

In Secs. II and III, two types of surface distortion were studied. At constant total volume (Sec. II), only fluctuations with a long wavelength can be stable. The local radii of curvature on this distortion are orders of magnitude larger than those of a crack tip. Distortions with a small local radius of curvature can be more stable than the initial state (Sec. III). In that case if a small amount of elastic energy has to be removed, e.g., by dissolution, they can develop into a critical crack.

At each applied stress, a minimum radius of curvature ρ_0 exists for a sine-type surface distortion. In that case there is zero change in total energy. For a fluctuation of the same depth, a decrease in energy is possible. The local radius is then larger than ρ_0. A minimum in total energy exists at $\rho_{\min} = 2\rho_0$. This is derived for small distortions ($2\pi a/\Lambda < 1$). For larger surface distortions, the actual values for ρ_0 and $\rho_{\min}$ deviate from those given in Eqs. (34) and (35). The idea, however, is the same: given the depth of a distortion, e.g., a crack, at a certain tip radius ρ_0 there is zero

energy change with length increase. At a larger tip radius, the total energy decreases with the same increase in the length of the crack.

The discrepancy between reaction velocity and energy criterion has already been discussed in Sec. IV: A high reaction velocity calls for a high local stress, i.e., a small radius of curvature. The energy criterion dictates a minimum radius ρ_0 at the tip. Both arguments have a part to play in the definition of the reaction path. This reaction path is defined by the driving force of the reaction, the (minimum) rate of entropy production. The actual reaction path is not calculated in this study. It is assumed that the maximum energy release rate determines this path.

Starting from a flat surface, lifetimes at constant ρ are given. They are boundary cases of the reaction path: at $\rho = \rho_0$, the reaction rate is relatively fast; there is no energy production because the total energy is constant. At $\rho = \rho_{min}$ ($= 2\rho_0$) the reaction rate is slower; the total energy decrease has its maximum. The maximum energy release rate will be somewhere between these two boundary cases. When starting from a flat surface, the calculated failure times [Eq. (49)] differ only by a factor of 2 at $\rho = \rho_0$ or $\rho = \rho_{min}$. In view of the initial condition, this result is not surprising: in this stage no stress concentration occurs, thus the slow reaction rates are equal. As in nearly all crack initiation and propagation problems, the lifetime is mainly determined by the (slowest) reaction rates in the initial stage. The difference in calculated failure times is thus due to small differences in the further stress corrosion process. In any case, an energy production rate needs $\rho > \rho_0$, thus a failure time longer than t_f calculated at ρ_0.

Doremus[21] has given a similar discussion for strength of materials with cracks. He noted the disagreement of Griffith's energy criterion [Eq. (37)] and Inglis' expression for tensile strength [Eq. (38)] for large cracks ($c \gg \rho$). In Griffith's fracture condition, there is zero change in total energy at a crack length increase dc. From the second law of thermodynamics, a minimum radius of curvature at the crack tip was derived. For the case of entropy production, $dU_{tot}/dc < 0$ was obtained [Eq. (37)]. The tip radius is larger than the minimum value. For failure, a local stress equal to the theoretical strength is needed. Due to the larger tip radius in the case of energy (entropy) production, the fracture load is larger than given by Griffith's fracture condition.

B. On the stress-corrosion limit

In the calculation of failure times in Sec. V, the reaction rate at the crack tip was assumed to be the rate-determining step. With the boundary condition of a constant radius of curvature at the tip, this means that the crack geometry as a function of time is well defined. The activation volume V_{calc} is stress dependent, but also strongly dependent on the initial geometry [Eqs. (53) and (58)]. For pristine optical fibers with a typical value of 4 GPa for the failure stress (Table I), the stress-dependent term $4RT/\sigma_a$ contributes about 2.5 cm^3/mol to V_{calc}.

Suppose now we have a small surface distortion defined by tip radius ρ_i and depth c_i. This may be an elliptical (surface) crack. The stress distribution around an elliptical hole

is given by Inglis (see, e.g., Ref. 9). A combination of this stress distribution and the stress corrosion rate [Eq. (2)] gives the time evolution of the crack geometry, and thus of the tip radius. Except for very small applied tensile stress, the tip radius decreases continuously. Stability considerations (Sec. III) resulted in a lower limit for the tip radius. It depends on the applied stress [Eq. (35)]: larger radii for lower stresses. If the tip radius approaches the lower limit, the stress corrosion rate at the tip is no longer the rate-determining step. A corrosion rate in another direction, needed to maintain the tip radius above the critical value ρ_0, defines the crack velocity. At the tip, the velocity is necessarily lower than given by (2).

From the initial tip radius ρ_i of an existing distortion, a critical stress value can be calculated [Eq. (35)]. Above this stress, tip sharpening occurs in the initial stage of the stress-corrosion reaction. The initial stage of the stress-corrosion reaction mainly determines the lifetime. The stress dependence of this lifetime is nearly equal for the cases with constant and decreasing tip radius [Eq. (58)], $q = 2$ or 4. Below this critical stress, the stress-corrosion reaction is no longer determined by the reaction velocities at the crack tip. The overall increase of the size of the surface distortion is smaller than expected from the stress at the tip. The stress dependence of the failure time, as given in Sec. V, is a conservative estimate. Below the critical stress the value for $(d \ln t_f/d\sigma_a)$ determined from the experiments are expected to be larger than V_{calc}.

In Eqs. (55) and (56) a more general expression for the lifetime is derived. From these expressions the expected slopes of the lifetime plots are calculated. From a plot of stress σ_a as a function of $\ln(t_f)$, V_{calc} [Eq. (51)] is obtained. It shows a strong dependence on the initial crack geometry [Eq. (58)]. The term in square brackets is nearly constant. It depends on q, and has a value between 1 and 4. Comparing values for the first and second terms in Eq. (58) it must be noted that for large values of X_i the stress σ_a is small in practical situations.

V_{calc} is derived for the case where the corrosion rate at the tip of the distortion (or crack) controls the rate of length increase. When this condition is no longer true (due to energy restrictions), the experimental slope $(d \ln t_f/d\sigma_a)$ will be larger than V_{calc}. A fatigue limit is approached.

The fatigue parameter n [Eq. (60)] is shown to depend on the local stress σ_l at the tip of the distortion. For smaller local stress a lower n value is obtained. n is not a constant. Like V_{calc}, n obtained from experiments may differ from the values obtained from Eq. (60) when a fatigue limit is approached at low stresses.

In lifetime measurements, e.g., on optical fibers, very low initial "crack growth velocities" are expected ($< 10^{-16}$ m/s). At these velocities the local stress is relatively low. For these low stresses a low value for n is expected from Eq. (60). For optical fibers many values for the fatigue parameter n are reported.[22] In many cases the n value increases with decreasing stress, thus giving larger lifetimes. It is assumed that in these cases a fatigue limit is approached. When a drastic decrease of n with increasing lifetime is observed, a competing chemical reaction may be active.[23]

C. Comparison with K_I models

In the lifetime prediction of stressed samples with large cracks ($c \gg \rho$) the stress intensity factor $K_I = Y\sigma_a \sqrt{c}$ [Eq. (1)] is often used as a parameter. It is used in the exponential expression (42),[15] and in the power law $v = AK_I^n$.[1] A comparison of $K_I = Y\sigma_a \sqrt{c}$ and Inglis' relation $\sigma_l = \sigma_a \times (1 + 2\sqrt{c/\rho})$ shows that K_I can be written as

$$K_I = Y\sigma_l \sqrt{\rho}/2. \tag{61}$$

At $K_I = K_{lc}$ the local stress σ_l is equal to the theoretical strength $\sigma_{\rm th}$.

The theory presented in this paper shows two important points that are neglected in the lifetime predictions of K_I-based models:

(1) The stress intensity K_I is defined for large cracks ($c \gg \rho$). For large cracks, the first term in Inglis' stress concentration relation is neglected. For small distortions ($c \simeq \rho$), this term, which is not taken into account in K_I, is not negligible. Starting from a flat surface ($c_i = 0$), it is shown in Eqs. (49) and (51) that it is mainly this first term of Inglis' relation that determines the stress dependence of the lifetime. The term in square brackets [Eq. (46)] is due to the second term in Inglis' relation. For cracks with $c \simeq \rho$, both terms contribute to the stress dependence of the lifetime [Eqs. (54) and (58)]. Only at large c/ρ ratios the contribution of the first term becomes insignificant.

(2) Expression (61) shows that K_I depends on the tip radius ρ. The theoretical strength $\sigma_{\rm th}$ of a material is determined by the bond strength and is thus constant for a given material. When K_{Ic} is a material constant, radius ρ is assumed to be constant. For brittle materials, like fused silica, ρ is small (< 1 nm).[13] Using K_I as a parameter in the stress corrosion reaction implies a reaction path at constant tip radius ρ.

For a small distortion ($2\pi a/\Lambda < 1$) the stress dependence of for stable surface distortions is clearly shown [Eqs. (34) and (35)]. This stress dependence dictates a reaction path: for smaller external forces, distortions with larger tip radii are used. This has influence on in the stress dependence of the failure time which is not taken into account in K_I models.

D. On the surface energy

In the discussion on the stability the surface energy term was introduced as γA, where γ is the specific surface energy. For liquids the surface energy and surface tension are equal; a surface increase means a larger amount of atoms on the outer surface. For solids, the surface energy and the surface tension are different in magnitude.[24] Here an increase in surface area can be produced also by stretching chemical bonds; the amount of surface atoms does not change. Therefore, the surface energy term of the stressed fiber may differ from that of the stress-free sample. This correction is not taken into account, neither in the present investigation, nor in the cited references.[16,25–27]

In the discussion on the reaction velocity the surface energy term has to be taken into account in the activation energy. This is done in Thomson's paper.[25] In Ref. 16 the contribution of the surface energy is assumed to be constant, and incorporated in the zero-stress activation energy E^*. In the lifetime descriptions used in this paper, the surface energy is not explicitly taken into account. Also here it may be taken as incorporated in the zero-stress activation energy E_a.

Charles and Hillig[26] introduced the surface energy in a term $\gamma V_m/\rho$, where V_m is the molar volume and ρ the radius of the crack tip. This term is used[27,28] to describe the influence of γ on crack blunting. It will be shown that the introduction of the term $\gamma V_m/\rho$ in the activation energy is based on nonvalid arguments. Suppose we have a stress-free cylindrical sample of radius r and surface energy γ. An unit length of this sample has volume $V = \pi r^2$ and a cylinder surface area $A = 2\pi r$. A radial compression of the material gives a lower surface area and a lower surface energy. The elastic energy increases. For a compressive strain ϵ the elastic energy is $\epsilon^2 E/2$ (E is Young's modulus). The free energy has a minimum at strain $\epsilon = -\gamma A/EV$. For the given case the free energy per mole is equal to $1/2(\epsilon^2 EV_m)$, the increase in elastic energy, and can be approximated with $\gamma V_m \Delta(1/r)$. The term $\gamma V_m/\rho$ results thus from the minimization of the total energy (the sum of elastic energy and the surface energy) when the initial state is not stressed.

For an already stressed sample, e.g., an external loaded fiber with initial strain ϵ_0, the total elastic energy has to be taken into account in the free-energy minimization. At the minimum in the total free energy the free energy decrease is given by $1/2[EV_m(\Delta\epsilon)^2]$, where $\Delta\epsilon = (\gamma A/EV) - \epsilon_0$. This is much smaller than $\gamma V_m \Delta(1/r)$, given for the stress-free case. From these arguments it is concluded that the term $\gamma V_m/\rho$ introduced by Charles and Hillig[26] is based on nonvalid arguments: the stressed initial state is not taken into account in this term.

In the study on the stability of a surface distortion in this paper the stressed initial state is taken into account. It is shown that the surface energy γ and the tip radius ρ of the distortion are related at the minimum of the total energy [Eq. (34)].

E. Final remarks

Within the present model the surface energy plays an important role. The magnitude of this quantity can vary.[11] A siloxane (Si-O-Si) surface is obtained when silica is treated at high temperatures ($> 600\,°C$). Hydration of siloxane gives silanol (Si-OH) groups. This decreases the surface (excess) energy. This formation of silanol groups is a slow process. It is likely that a freshly prepared silica fiber has a siloxane surface.

Due to physisorption and/or chemisorption of other constituents on the surface, the energy state of the surface also changes. The heat of wetting of a silanol surface, for instance, differs markedly from that of a siloxane surface. In this view, the state of the surface (siloxane/silanol) and other surface conditions, like the amount of adsorbed water, are important for the strength/lifetime characteristics of a fiber.

The process for material removal at the distortion is not specified here. Local dissolution was a suggestion. When the process is not clearly specified, the total energy description is

not a complete thermodynamic description. In a thermodynamic description, the entropy has to be taken into account. Only in that case the actual reaction path can be calculated.

A flat surface is proposed as initial condition. A distortion of this surface can ultimately lead to failure of the stressed sample. Nothing is said about how such small distortions originate. It is only assumed that they are present.

Stable surface distortions have nanometer dimensions. Macroscopic models are used to describe fluctuations at atomic dimensions.

To simplify calculations, fluctuations over the whole circumference of the fiber were studied in Secs. II and III. Fluctuations that are not over the whole circumference lead to the same type of results; their numerical values will be slightly different.

VIII. CONCLUSION

A model has been presented for the failure of a perfect fiber. Within the model it is assumed that the initial state is a flat surface. Surface distortions develop during the test. Starting from a flat surface, a fluctuation of the surface is under certain conditions stable with respect to the initial state of a stressed fiber. When small amounts of material are removed from the stressed system, constant local radii of curvature are obtained as stability criteria. For an optical fiber they are smaller than 1 nm. The surface distortions can grow to critical cracks, leading to material failure. The fiber fails under tensile stress, although no initial crack was present. For special cases, failure times are calculated.

Using this model, expressions for the lifetime under applied stresses are calculated. This is done for cases with and without initial cracks. From these expressions it is shown that the fatigue parameter n, used to describe stress corrosion empirically, is not a constant, but depends on the local stress. This dependence resolves the observed discrepancy in n value between bulk silica and silica fibers.

The expressions derived in this paper are used in the interpretation of lifetime experiments on optical fibers with various coatings,[22] and will be discussed in forthcoming papers.

[1]S. W. Freiman, in *Glass, Science, and Technology*, edited by D. R. Uhlmann and N. J. Kreidl (Academic, New York, 1980), Vol. 5, Chap. 2.

[2]B. R. Lawn and T. R. Wilshaw, *Fracture of Brittle Solids* (Cambridge University Press, Cambridge, 1975), Chap. 1.

[3]P. W. France, M. J. Paradine, M. H. Reeve, and G. R. Newns, J. Mater. Sci. 15, 825 (1980).

[4]W. J. Duncan, J. Comm. Am. Ceram. Soc. 69, C132 (1986).

[5]S. Sakaguchi and T. Kimura, J. Am. Ceram. Soc. 64, 259 (1981).

[6]C. R. Kurkjian and U. C. Peak, Appl. Phys. Lett. 42, 251 (1983).

[7]A. S. Krausz and H. Eyring, *Deformation Kinetics* (Wiley, New York, 1975).

[8]S. Glasstone, K. J. Laidler, and H. Eyring, *The Theory of Rate Processes* (McGraw-Hill, New York, 1941), Chap. 8.

[9]S. P. Timoshenko and J. N. Goodier, *Theory of Elasticity*, 3rd ed. (McGraw-Hill, Kogakusha, Tokyo, 1970).

[10]G. J. Kynch, *Mathematics for the Chemist* (Butterworths, London, 1955).

[11]H. C. Chandan and D. Kalish, J. Am. Ceram. Soc. 65, 171 (1982).

[12]R. K. Iler, *The Chemistry of Silica* (Wiley, New York, 1975).

[13]S. Ito and M. Tomozawa, J. Am. Ceram. Soc. 65, 368 (1983).

[14]I. Prigogine, *Introduction to Thermodynamics of Irreversible Processes*, 3rd ed. (Wiley Interscience, New York, 1967).

[15]S. M. Wiederhorn and L. H. Bolz, J. Am. Ceram. Soc. 53, 543 (1970).

[16]S. M. Wiederhorn, E. R. Fuller, and R. Thomson, Metals Sci. 14, 450 (1980).

[17]N. P. Bansal and R. H. Doremus, *Handbook of Glass Properties* (Academic, Orlando, FL, 1986), Chap. 12.

[18]R. J. Charles, J. Appl. Phys. 29, 1554 (1958).

[19]S. Sakaguchi, Y. Sawaki, Y. Abe, and T. Kawasaki, J. Mater. Sci. 17, 2878 (1982).

[20]P. C. P. Bouten, *Proceedings of the 13th European Conference on Optical Communications*, Helsinki, 13–17 Sept., 1987, pp. 223–224

[21]R. H. Doremus, J. Appl. Phys. 47, 1833 (1976).

[22]J. D. Helfinstine and F. Quan, Optics Laser Comm. 14, 33 (1982).

[23]P. C. P. Bouten, thesis, University of Technology, Eindhoven, 1987.

[24]R. G. Linford, *Solid State Surface Science*, edited by M. Green (Dekker, New York, 1973), Vol. 2, Chap. 1, pp. 1–152.

[25]R. Thomson, J. Mater. Sci. 15, 1014 (1980); E. R. Fuller and R. Thomson, J. Mater. Sci. 15, 1027 (1980).

[26]R. J. Charles and W. B. Hillig, *Symp. sur la Resistance Mechanique du Verre et les Moyens de l'Ameriorer*, Compte rendu, Florence, 25–29 Sept. 1961 (Union Scientifique Continentale du Verre, Charleroi, 1962).

[27]W. B. Hillig and R. J. Charles, *High Strength Materials*, edited by V. F. Zackay (Wiley, New York, 1965), Chap. 17, pp. 682–705.

[28]T. A. Michalske, *Fracture Mechanics of Ceramics*, edited by R. C. Bradt, A. G. Evans, D. P. H. Hasselmann, and F. F. Lange (Plenum, New York, 1983), Vol. 5, pp. 277–289.